



Flt3L-dependence helps define an uncharacterized subset of murine cutaneous dendritic cells

Citation

Mollah, Shamim, Joseph Dobrin, Rachel Feder, Sze-Wah Tse, Ines Matos, Cheolho Cheong, Ralph M. Steinman, and Niroshana Anandasabapathy. 2014. "Flt3L-dependence helps define an uncharacterized subset of murine cutaneous dendritic cells." *The Journal of investigative dermatology* 134 (5): 1265-1275. doi:10.1038/jid.2013.515. <http://dx.doi.org/10.1038/jid.2013.515>.

Published Version

doi:10.1038/jid.2013.515

Permanent link

<http://nrs.harvard.edu/urn-3:HUL.InstRepos:13454847>

Terms of Use

This article was downloaded from Harvard University's DASH repository, and is made available under the terms and conditions applicable to Other Posted Material, as set forth at <http://nrs.harvard.edu/urn-3:HUL.InstRepos:dash.current.terms-of-use#LAA>

Share Your Story

The Harvard community has made this article openly available.
Please share how this access benefits you. [Submit a story](#).

[Accessibility](#)

Published in final edited form as:

J Invest Dermatol. 2014 May ; 134(5): 1265–1275. doi:10.1038/jid.2013.515.

Flt3L-dependence helps define an uncharacterized subset of murine cutaneous dendritic cells

Shamim Mollah^{3,^}, Joseph Dobrin^{1,2,^}, Rachel Feder^{1,2}, Sze-Wah Tse⁴, Ines Matos^{1,2}, Cheolho Cheong⁴, Ralph M. Steinman^{1,2}, and Niroshana Anandasabapathy^{1,2,5,*}

¹Laboratory of Cellular Physiology and Immunology, Rockefeller University New York, NY

²Christopher H. Browne Center for Immunology and Immune Diseases Rockefeller University New York, NY

³Hospital Informatics, Rockefeller University New York, NY

⁴Laboratory of Cellular Physiology and Immunology, Institut de recherches cliniques de Montréal (IRCM)

⁵Department of Dermatology/Harvard Skin Disease Research Center, Brigham and Women's Hospital, Boston, MA 02115, USA

Abstract

Skin-derived dendritic cells (DC) are potent antigen presenting cells with critical roles in both adaptive immunity and tolerance to self. Skin DC carry antigens and constitutively migrate to the skin draining lymph nodes (LN). In mice, Langerin-CD11b[−] dermal DC are a low-frequency, heterogeneous, migratory DC subset that traffic to LN (Langerin-CD11b-migDC). Here, we build on the observation that Langerin-CD11b[−] migDC are Fms-like tyrosine kinase 3 ligand (Flt3L) dependent and strongly Flt3L responsive, which may relate them to classical DCs. Examination of DC capture of FITC from painted skin, DC isolation from skin explant culture, and from the skin of CCR7 knockout mice which accumulate migDC, demonstrate these cells are cutaneous residents. Langerin-CD11b-Flt3L responsive DC are largely CD24(+) and CX₃CR1^{low} and can be depleted from Zbtb46-DTR mice, suggesting classical DC lineage. Langerin-CD11bmigDC present antigen with equal efficiency to other DC subsets *ex vivo* including classical CD8α cDC and Langerin+CD103+ dermal DC. Finally, transcriptome analysis suggests a close relationship to other skin DC, and a lineage relationship to other classical DC. This work demonstrates that Langerin- CD11b[−] dermal DC, a previously overlooked cell subset, may be an important player in the cutaneous immune environment.

INTRODUCTION

As the primary barrier between the body and the outside world, the skin is a unique immune organ. The importance of cutaneous immunity is demonstrated several ways. First,

*Corresponding author, Harvard Institute of Medicine Room 660, Boston MA 02115. Phone (617) 525-8342, nanandasabapathy@partners.org.

[^]These authors contributed equally to this work

CONFLICT OF INTEREST: Ralph Steinman was on the scientific advisory board and held stock options in Celldex Therapeutics.

successful vaccination strategies rely on delivery of vaccine antigens to the skin including vaccinia (Liu *et al.*, 2010) and dermally-delivered influenza (Kenney *et al.*, 2004). Second, innate immune adjuvants that act on the cutaneous immune network (imiquimod, resiquimod) can lead to the regression of lentigo maligna and superficial spreading basal cell carcinomas (Schon and Schon, 2008). Third, steady state immune surveillance is critical to prevent skin cancers as evidenced by the markedly increased incidence of neoplasia observed in renal transplant recipients maintained on immunosuppressive agents (Clark, 2010). Despite the immune-responsive nature of skin cancers and potential for skin resident immune cells to mediate adaptive responses to cancer and infection, therapies have not been generated to prevent skin cancer formation. Improved understanding of adaptive immunity in the cutaneous environment is needed.

Adaptive cutaneous immunity depends on Dendritic Cells (DC) that abundantly populate the skin and skin draining LN. DC are low-frequency hematopoietic cells, specialized at antigen presentation. DC educate T cells to respond to tumor and microbial antigens, control the developing immune response, and maintain long-term immune memory to tumors and infections. In the non-inflamed state human skin contains 4 known phenotypically distinct subsets of DC (Haniffa *et al.*, 2012; Teunissen *et al.*, 2012), while murine skin contains 5 (Henri *et al.*, 2010). These DC continuously migrate from skin to the draining LN and are collectively termed migratory (migDC). Given such phenotypic heterogeneity amongst skin DC, increasing efforts are aimed at identifying their functional and developmental attributes and correlating these with well-described DC subsets in other tissues.

Classical-DC are lymphoid and non-lymphoid DC that derive from pre-DC originating from a common bone marrow precursor (Common DC Precursor). The term classical is used to distinguish these populations from plasmacytoid DC (PDC) (Merad *et al.*, 2013) and monocyte-derived DC which develop in the setting of inflammation. Classical DC broadly may be divided into CD11b⁺ and CD11b[−] populations. Classical DC that are LN and spleen resident and are CD11b[−] also express CD8α and CD205 (termed CD8α⁺ cDC), while CD11b⁺ LN and spleen resident DC lack expression of CD8α[−] (termed CD11b⁺ cDC). In peripheral tissue such as skin CD11b[−] and CD11b⁺ may be additionally divided based on other markers such as CD103 and Langerin.

In draining LNs, cell-surface expression of CD11c and MHCII is used to separate the 3 major DC groups: plasmacytoid DC, LN resident classical DC (cDC), and migratory DC (migDC). MigDC include some DC of classical lineage that are CD11b[−] and CD11b⁺ such as Langerin⁺CD103⁺CD11b[−] DC and Langerin[−]CD11b⁺ DC respectively (Ginhoux *et al.*, 2009). MigDC also include Langerhans cells (LC) of the epidermis, whose origin is distinct and which are not seeded from pre-DC, but derive instead from radioresistant precursors (Helft *et al.*, 2010). Though an additional migratory population of CD11b[−] cells was previously identified in skin (Langerin[−]CD11b[−]) (Henri *et al.*, 2010), these cells have been largely overlooked and incompletely characterized because they exist in low abundance in other peripheral tissue such as the lung and mucosa, though they comprise a significant fraction of DC from the skin.

Some DC are functionally specialized at cross-presentation, the major pathway to present viral and tumor antigens. These DC have unique properties that make them attractive cellular targets for vaccination (Poulin *et al.*, 2010). When mature, they are superior to cross-present exogenous antigens on MHC I, ingest dead or dying cells, and produce IL-12 in response to innate and T cell derived cues (Shortman and Heath, 2010; Yamazaki *et al.*, 2008). In skin, Langerin+ CD103+ DC cross-present antigens, and CD8 α +CD11b– DC, which also express the C-type lectin CD205 (CD8 α DC), cross-present antigens in lymphoid organs. In skin and other epithelial tissue, CD103+ DC, cross-present antigens from cytolytic viruses and epithelial pathogens (Bedoui *et al.*, 2009) including influenza (Helft *et al.*, 2012), herpes virus (Bedoui *et al.*, 2009), and erosive candida (Igyarto *et al.*, 2011). Several lines of evidence suggest that other skin DC beyond Langerin+ CD103+ DC may have an important role in priming to vaccines and pathogens. Langerin+ CD103+ DC are not required in dermal vaccine administration (Flacher *et al.*, 2012). Furthermore, residual antigen presentation capacity to cutaneous pathogens including erosive candida (Igyarto *et al.*, 2011) and vaccinia (Seneschal *et al.*, 2013) is observed in the absence of Langerin+CD103+ DC. These data suggest that another DC subset may cross-present antigens locally in the skin and skin-draining LN.

Flt3L, a DC hematopoietin, and its receptor (Flt3, FLK2) regulate classical DC homeostasis of both DC in lymphoid organs and DC at, or arriving from, peripheral tissue (CD103+ DC in skin and lungs) (Waskow *et al.*, 2008, Liu *et al.*, 2009). Migratory Langerin+ CD103+ DC, CD8 α lymphoid resident cDC, and human BDCA3+ cross-presenting DC share developmental dependence on Flt3L (Haniffa *et al.*, 2012, Ginhoux *et al.*, 2009). Flt3L treatment biases cDC development to cross-presenting DC (Bozzacco *et al.*, 2010). Flt3L expansion of DC has helped identify very infrequent but functionally important DC at epithelial sites- such as blood brain barrier (Anandasabapathy *et al.*, 2011) and aortic intima (Choi *et al.*, 2011). However Flt3L dependence has not been used to characterize infrequent DC in the skin or migDC in the skin draining LN.

Here we analyze the cutaneous residence, migratory properties, developmental dependence, transcriptome, and functional properties of a cutaneous Langerin-CD11b– migratory DC subset (abbreviated Langerin- CD11b– migDC). Our data suggest this subset is heterogeneous but contains highly Flt3L-responsive DC with potent antigen presentation capacity. We demonstrate Langerin-CD11b– migDC share many features with other classical Flt3L-dependent DC.

RESULTS

Langerin-CD11b– migDC are Flt3L dependent

We examined the expansion of migDC in the skin draining LNs of mice in the presence and absence of *in vivo* Flt3L treatment. MigDC can be gated as CD11c^{int} and IAIE (MHCII)^{hi} and further divide into Langerin+ known DC subsets including Langerin+ CD103+ DC, and Langerin+ CD103– DC (which includes Langerhans cells). Langerin- migDC subsets include Langerin-CD11b+ DC and Langerin-CD11b-DC (Henri *et al.*, 2010). (Figure 1A, and gating in Figure S1A). In C57BL/6 mice (Figure 1A) and Langerin GFP mice (Figure 1B) treated with Flt3L, we observed a major expansion of LN migDC within the Langerin-

compartment, comprised of both CD11b⁺ and CD11b[−] cells. This was intriguing because our lab and others have shown a parallel expansion of CD11b[−] (CD8α⁺) and CD11b⁺ (CD8α[−]) cDC in lymphoid tissue after Flt3L treatment (Bozzacco *et al.*, 2010). LN DC subsets numbers were quantitated from mice Flt3L treated, untreated, and knockout mice (Figure 1C). Langerin-CD11b⁺ and Langerin-CD11b[−] subsets were expanded most significantly by Flt3L treatment. Flt3L loss affected Langerin⁺CD103⁺ DC, and Langerin-CD11b⁺ and Langerin-CD11b[−] subsets.

CD11b[−] migDC are skin resident and traffic to the skin draining LN

To ascertain if Langerin-CD11b[−] cells migrated to the LN from skin, or were a contaminant from LN resident populations such as CD8α cDC, we examined skin explants in which DC are directly isolated from skin. CD11b[−] cell were present and expanded with Flt3L in “crawlout” DC isolation from skin (gating, Figure S1B). We established this in several models- in Flt3L doxycycline-inducible mice (Manfra *et al.*, 2003) (Figure 1D), recombinant Flt3L-treated Langerin GFP mice (Figure 1E, S1B), recombinant Flt3L-treated C57Bl/6 mice (Figure S1C), and Flt3L secreting B16 tumor treated mice (Figure S1D). In cDC Flt3L creates bias to CD8α CD205⁺ cross-presenting cDC. Analysis of CD205⁺ expression on migDC explants revealed Langerin-CD11b[−] DC contained both CD205^{high} and CD205^{low} cells in the steady state. However, a higher percentage of CD11b[−] cells are CD205^{high} after treatment with Flt3L (Figure 1F).

Skin migDC depend on CCR7 for migration to LN (Forster *et al.*, 1999). To further validate that Langerin-CD11b[−] cells in LN have migrated from the skin, we examined CCR7^{−/−} mice treated with Flt3L vs. untreated controls. Irrespective of Flt3L treatment, LNs from CCR7 knockout mice lack cells within the CD11c^{int}IAIE^{hi} DC migratory gate (Figure 2 A, upper panel). MigDC subsets including CD11b[−] cells preferentially accumulated in skin explants and expanded with Flt3L locally in skin (Figure 2A, lower panel). When FITC is applied with a contact-sensitizing agent to the epidermis of mice, migDC rapidly transport FITC from skin to skin draining LN. FITC label was present only in the IAIE^{hi} migratory cells (Figure 2B). Examination of FITC⁺ migDC vs. all migDC demonstrated an enhanced representation of FITC⁺ Langerin-CD11b[−] cells during inflammation and FITC painting. Several populations of DC transported FITC to the skin draining LN, yet a greater fraction of Langerin-CD11b[−] and Langerin-CD11b⁺ DC subsets were present that labeled with FITC when compared to all migDC after FITC painting (Figure 2B). These data suggest Langerin-CD11b[−] DC like other migDC can transport FITC from the skin to the skin draining LN. To visualize Langerin-CD11b[−] DC directly in skin immunofluorescence staining was performed in Flt3L treated and untreated mice. LC were marked in the epidermis (Langerin⁺ CD11b⁺ CD11c⁺). Contained within dermal CD11c⁺ cells, we observed Langerin-CD11b⁺ DC, Langerin-CD11b[−] DC, and Langerin⁺CD11b[−] cells (Figure 2C).

Langerin-CD11b[−] migDC are heterogenous but contain a Flt3L responsive CD24^{hi} CX3CR1^{low} DC population

Given that CD205^{high} and CD205^{low} expressing cells were present in the steady state within Langerin- CD11b[−] migDC, yet enhanced numbers of CD205^{high} expressing cells were

noted after Flt3L treatment, we speculated that the Langerin-CD11b[−] subset might be heterogeneous in the steady-state. To address this we examined CD24 expression, an additional marker for CD8α cDC, on migDC before and after Flt3L treatment. We observed Flt3L treatment expands the percentage of Langerin-CD11b[−] cells expressing CD24 in the LN from about 40% to almost 80% with a more modest and variable percentage expansion in skin (Figure 3A, S1C–D). We also noted that in skin and LN an increase in the absolute number of Langerin-CD11b-CD24⁺ cells occurred after Flt3L and a correspondingly higher ratio of Langerin-CD11b-CD24⁺ cells in Flt3L treated vs. control mice (quantitation, S2). An increased percentage of CD24⁺ cells after Flt3L was also observed on CD8α + cross-presenting cDC in LN. Langerin⁺ DC subsets have high CD24 expression and CD11b⁺ DC have lower CD24⁺ levels at baseline. In CD11b⁺ migDC, CD24⁺ percentage was not dramatically altered after Flt3L treatment in LN and skin (Figure 3A and S1C–D). These data suggest Flt3L expands CD24⁺ Langerin-CD11b[−] cells. In contrast, during FITC painting in the presence of a pro-inflammatory contact-sensitizing agent we observe the expanded CD11b[−] population is predominantly CD24^{low} (Figure S1E).

To further investigate Langerin-CD11b[−] heterogeneity, we examined the expression of CX₃CR1 using CX₃CR1-GFP reporter mice (Jung *et al.*, 2000). The chemokine receptor CX₃CR1 (fractaline) is abundantly expressed on CD11b⁺ LN resident cDC and largely absent from the majority of CD8α LN resident cDC, which helps to distinguish these 2 subsets (Figure 3B). The small fraction of CD8α⁺ DC which express CX₃CR1, lack cDC capacity for IL-12 secretion, cross-presentation of antigen, and resemble CD8α cDC (Bar-On *et al.*, 2010). After Flt3L treatment, CD8α⁺ CD24^{hi} CX₃CR1^{low} cDC (red, upper) remain well-distinguished from CD11b⁺ CD24^{low} CX₃CR1^{hi} cDC (blue, upper) (Figure 3B). In the steady state Langerin-CD11b[−] cells are approximately 50% CD24^{high} CX₃CR1^{low} as compared to Langerin-CD11b⁺ migDC which were predominantly CD24^{low} CX₃CR1^{hi} in the steady state (lower, left). After Flt3L, 70% of Langerin-CD11b[−] migDC became CD24^{hi} CX₃CR1^{low} suggesting Flt3L expands this population selectively (lower, right). Collectively these data suggest in the steady state Langerin-CD11b cells are heterogeneous but Flt3L selectively expands a CD24^{hi} CX₃CR1^{low} subset, distinct from CD11b⁺ CD24^{low} CX₃CR1^{hi} migDC.

Langerin-CD11b[−] migDC, like other cDC, depend on the transcription factor Zbtb46

To further characterize Langerin-CD11b[−] cells we took advantage of recently generated Zbtb46-diphtheria toxin receptor (DTR) mice which allows specific depletion of cDC and their precursors, but does not affect PDCs, monocytes, or macrophages (Meredith *et al.*, 2012a; Meredith *et al.*, 2012b; Satpathy *et al.*, 2012). At 24 and 48 hours post DT treatment an overall gross reduction in total number of LN resident cDCs was observed as expected (Figure 4A, gating S3A). MigDC were also rapidly depleted (Figure 4B). Langerin-CD11b[−] cells were efficiently depleted along with other cDC in the LN (Figure 4B) and in skin (4C and S3B) with few residual cells left. These data suggest Langerin-CD11b[−] cells are a Zbtb46-expressing classical DC subset that shares the same origin as cDC.

Langerin-CD11b⁺ migDC perform key DC functions

To further examine whether the Langerin-CD11b⁺ subset could perform key DC functions we sorted CD8 α LN resident cDC and several migDC subsets from Langerin GFP mice treated with Flt3L. We tested individual DC subsets (C57BL/6) in the mixed leukocyte reaction (MLR) using T cells from BALB/c mice. All DC types could effectively stimulate allogeneic T cells, including Langerin-CD11b⁺ migDC (Figure 5A–B). Additionally we sorted and cultured DC subsets with titrated doses of OVA protein and CD8⁺ –1 transgenic T cells. Again Langerin-CD11b⁺ DC were comparable to other LN resident and migDC subsets at OVA-antigen presentation to CD8 T cells *ex vivo* (Figure 5C–D, gating and representative flow data Figure S4). These data suggest Langerin-CD11b⁺ migDC perform equivalent antigen presentation of OVA to CD8⁺ T cells when compared to other DC, including CD8 α and CD103⁺ Langerin⁺ DC.

Langerin-CD11b⁺ migDC relate closely to other skin DC and other cDC and express core DC signature genes

To further address the relationship of individual migDC populations to each other and to cDC in LN we performed transcriptome analysis. We also included two additional subsets of LN DC in our analysis obtained from LPS treated mice: DC-SIGN⁺ monocyte-derived DC and CD205⁺ DC (Cheong *et al.*, 2010) and peritoneal macrophages. Using principal component analysis (PCA) we identified four distinct clusters (*data not shown*): one cluster was formed by migDC subsets including Langerin CD103⁺DC, Langerin-CD11b⁺DC, and Langerin-CD11b⁺ DC, consistent with prior work suggesting tissue DC cluster together (Miller *et al.*, 2012). Hierarchy analysis (dendrogram) (Figure 6A) revealed close relatedness of cutaneous Langerin-CD11b⁺ and Langerin-CD11b⁺ subsets to each other, and to Langerin+CD103⁺ and CD8 α cDC when compared against macrophages and LPS-treated DC subsets.

Recent studies have defined a “core-DC gene signature” when comparing multiple cDC to macrophages (Miller *et al.*, 2012). By heat map analysis we analyzed the expression of many of these previously defined core DC genes in our subsets, shown as a relative fold expression against macrophages (Figure 6B). Many core DC genes including Flt3, Ccr7, and Zbtb46 were upregulated in all DC subsets examined including Langerin-CD11b⁺ migDC. Heat map comparison of additional selected DC genes was also performed across all populations (Figure 6C). These include Irf8, Clec9A, Ly75 (CD205, Dec205), Stat3, Zbtb46, Flt3, and Ccr7. Irf8, a transcription factor necessary for CD8 α (and its equivalents) lineage development (Seillet *et al.*, 2013), was observed at the highest expression intensity in CD8 α ⁺ and Langerin+CD103⁺ and in CD205⁺ DC despite LPS treatment. CD11b⁺ migDC levels of Irf8 were intermediate but higher than in CD11b⁺ DC, DC-Sign⁺ LPS-treated monocyte-derived DC, and macrophages.

DISCUSSION

This study characterizes a previously identified skin resident subset of immune cells (Henri *et al.*, 2010), that we now demonstrate are migDC sharing many properties to cDC including Flt3L and Zbtb46 dependence. The current study builds on prior work in which Langerin-

CD11b[−] DC along with several other subsets were isolated from skin and skin draining LN of mice. Previously Langerin-CD11b[−] DC were noted to share division and repopulation kinetics along with other dermal DC such as Langerin⁺CD103⁺ DC suggesting a common precursor (Henri *et al.*, 2010), yet have been largely overlooked given the cross-presenting properties of Langerin⁺CD103⁺ DC. Here we provide a dedicated characterization of Langerin-CD11b[−] migDC based on developmental, phenotypic, and functional DC criteria establishing these cells as a distinct DC subset by transcriptome analysis and relating them to other Flt3L-dependent classical DC subsets, distinct from monocytes and macrophages.

We establish Langerin-CD11b[−] are heterogeneous in the steady state but contain a highly Flt3L-dependent and responsive population. Markedly reduced dermal Langerin-CD11b⁺ and Langerin-CD11b[−] DC subsets were gated from LN in Flt3L^{−/−} mice. Flt3L treatment preferentially expanded Langerin-CD11b[−] and Langerin-CD11b⁺ dermal DC subsets in the LN, and in the skin by crawlout explant. This may parallel spleen and BM where Flt3L expanded DC consistently divide into CD11b^{hi} DC subsets (CD8α-cDC equivalents) and CD11b^{low} CD24^{hi} SIRP α^{low-intermediate} (CD8α + cDC equivalents) (Naik *et al.*, 2005). Langerin-CD11b[−] Flt3L responsive DC, like classical CD8α + CD11b[−] cDC, are CD24⁺ and CX₃CR1^{low} and are efficiently depleted in DT-treated Zbtb46 DTR mice. Like other migDC, we determine Langerin-CD11b[−] are CCR7 dependent, are skin residents by explant and FITC painting, expand locally in the skin in response to Flt3L, and may be visualized in the dermis. Langerhans cells are radio-resistant, do not express Flt3 (Ginhoux *et al.*, 2012), and were not anticipated to expand. These data suggest Langerin- DC comprise the majority of the 14-fold Flt3L based CD11c⁺ expansion previously noted in dermis (Esche *et al.*, 1999). Though our study was conducted in mice, Flt3L dependence and Flt3L expansion of local cutaneous DC subsets is of particular importance to the cancer vaccine arena as current and prior translational efforts aim to deliver cancer antigens to DC after subcutaneous administration of Flt3L.

We observed Langerin-CD11b[−] DC from mice treated with Flt3L performed allo-MLR and cross-presentation to OVA at equal efficiency to LN resident cDC. This suggests an efficient role in antigen presentation and bona fide DC function. This may be of significance to priming against erosive candida and cytolytic viruses where residual T cell priming by DC occurs even in the absence of Langerin⁺CD103⁺ dermal DC, yet no other DC subset in skin has been identified as responsible for residual priming. However strictly *ex vivo* analysis of DC function is somewhat limited by the fact that migDC mature in culture after leaving the skin and distinct individual *in vivo* roles of cutaneous DC subsets are still incompletely characterized. Current models of acute DC depletion (Langerin-DTR, CD11B-DTR, Zbtb46-DTR, and CD11c-DTR) cannot selectively isolate Langerin-CD11b[−] migDC at this time; therefore it will be difficult to immediately resolve their *in vivo* role in mediating cutaneous immunity. It is possible that when licensed to prime, DC subset activity in the skin could relate to specialization or non-redundant coverage of various pathogens. Differing susceptibility of DC subsets to infection may permit discrete roles in antigen presentation, as observed for tissue resident CD103⁺ DC vs. alveolar macrophages during influenza infection (Helft *et al.*, 2012).

We have determined migDC group together by hierarchy clustering. These data suggest three dermal DC subsets are closely related at the transcriptome level to each other and may suggest that tissue microenvironment impacts terminal DC differentiation. As such, Langerin+CD103+ DC group more closely with other migDC than with their lymphoid developmental and functional equivalents-CD8 α cDC. Perhaps in the steady state tissue resident migDC may act in concert. Intriguingly LN CD205+ cDC from LPS treated mice cluster with LPS-treated DC such as DC-SIGN+ monocyte-derived DC than to cDC. The dominant gene signatures relating these subsets in this context are likely related to LPS treatment.

A lack of clarity surrounding the function and development of diverse DC subsets present in the skin and skin draining LN has long hindered the development of vaccines and clinical therapeutics to skin cancer. This work suggests the previously overlooked Langerin-CD11b- DC subset contains a distinct, previously uncharacterized Flt3L-responsive migratory population with many properties of cDC. As such, Langerin-CD11b- DC may serve as a potential target of therapeutics aimed to enhance cutaneous immunity and as a mediator of the cutaneous immune response.

METHODS

Tissue Harvest and DC Cell Preparation

“Flt3L-treated” mice were injected by the intraperitoneal (IP) route with endotoxin-free (< 0.0064 EU/mg), GMP grade, recombinant human Flt3L (Celldex) at 10 μ g/mouse/day, diluted in sterile PBS vs. sterile PBS treated or untreated C57Bl/6 controls by IP injection. “Tumor treated” 8–12 week C57BL/6 F or Langerin-GFP mice were administered 5×10^6 murine Flt3L-secreting B16 melanoma tumor cells by subcutaneous injection. Doxycycline-inducible models of Flt3L induction have been previously characterized (Manfra *et al*, 2003). At 10–14 days of IP injection of Flt3L, approximately 10 mm tumor size, or after 8–12 days of doxycycline addition to drinking water, mice were sacrificed. Skin-draining LNs (inguinal, brachial, axillary, popliteal, and superficial cervical pooled) and spleen were isolated from individual mice. LNs and spleen were added to Collagenase D (400 U/ml, Roche) in Hanks’ Balanced Salt Buffer (Gibco) solution. LNs were teased apart and spleen were injected with this solution using a 22–23 gauge needle attached to a 3 mL syringe, and incubated for 25 minutes at 37°C (Steinman *et al.*, 1979). After incubation 0.5M EDTA was added to a final concentration of 10mM EDTA for disruption of DC:T cell complexes and the sample was further incubated for 5 min at 37°C. For spleen cell preparation, ACK lysis of red cells was performed. Undigested fibrous material was filtered through a 70 μ m cell strainer. Subsequent washes were performed with ice cold PBS with 2% fetal calf serum (FCS). For crawlout assay, individual ears were harvested, washed in 70% EtOH and both sides of ear halves were split dermal side down into R5-RPMI media with 10% FCS. Crawlouts were harvested in 6 well plates (one ear per well) leading to some variability in total cell counts across explants. At 72 hours cell suspensions were isolated and filtered. The pellet was washed twice, and incubated in Fc block with 2% rat serum prior to cell surface marker antibody staining.

Mice—C57BL/6 mice (B6) were purchased from Taconic Labs or bred at Rockefeller University. CCR7^{-/-} mice were bred at Rockefeller after purchase from Jackson and are described with respect to defects in the skin-derived DC migration (Martin-Fontecha *et al.*, 2008; Martin-Fontecha *et al.*, 2003). Langerin-GFP mice were generously provided by Bernard Malissen, bred as homozygotes at Rockefeller University, and have been previously described (Kissenpfennig *et al.*, 2005). CX₃CR1-GFP mice were purchased from Jackson and previously described (Jung *et al.*, 2000). Zbtb46-DTR mice were generously provided by Matthew Meredith and Michel Nussenzweig. Doxycycline-inducible Flt3L were kindly provided by Sergio Lira. All mice were housed in specific pathogen-free conditions. Protocols were approved by the Rockefeller University and Harvard University Animal Care and Use Committees.

DC isolation—For allo-MLR, OVA presentation, and microarray RNA isolation DC subsets were sorted from 5–10 pooled Flt3L treated Langerin-GFP mice per experiment. Following size, live/dead, and exclusion criteria (CD3, CD19, NK1.1 exclusion) DC subsets were sorted following the general gating schema depicted in S1a. DC-SIGN⁺ and CD205⁺ DC were sorted from the skin draining LNs of C57BL/6 mice 24 hours after intravenous injection of 5ug of LPS (Cheong *et al.*, 2010) and macrophages were isolated from peritoneum.

Immunofluorescence

Back skin from Flt3L treated (12 days) or untreated C57BL/6 controls was isolated and frozen in tissue-tek OCT (Sakura Finetek). 6-μm sections were cut by cryomicrotome (Leica) sectioning, air-dried and fixed in ice-cold acetone. Sections were pre-treated with endogenous avidin/biotin block (Invitrogen) and further blocked with 10% normal goat serum (Jackson ImmunoResearch Laboratories). Sequential immunofluorescence staining was performed using anti-langerin (clone 929F3, Dendritics), anti-CD11b (clone M1/70; Biolegend) and anti-CD11c (clone HL3, BD Biosciences) with the appropriate secondary antibodies (anti-rat IgG2a FITC (eBioscience), anti-rat IgG2b eFluor570 (eBioscience), and streptavidin-Alexa Fluor 647 (Invitrogen). Sections were mounted with Vectashield with DAPI (Vector labs). Images were acquired on a VS120 Whole Slide Scanner (Olympus) at 10X magnification using ASW software and analyzed using Olyvia software (Olympus).

Microarray analysis, normalization and data analysis

RNA samples were prepared by standard methods using Trizol (Invitrogen) and further purified using RNeasy MinElute clean up (QIAGEN). Purity analysis was done by nanodrop and Eukaryote Total RNA Pico Series II (Agilent). RNA was amplified and hybridized on the Illumina MouseRef-8 v2.0 Expression BeadChip. For subset analysis at least three replicates were analyzed from individual sorts to achieve statistical significance. Raw data from Illumina single color chips were analyzed with GeneSpring 12.5. Intensities below background were replaced with the average background over all samples. Quantile normalization was applied to have a common distribution of intensities, followed by log₂ transformation. Normalized values were baseline transformed to the median of all samples. Normalized data were filtered to eliminate probes with low expression with a coefficient of variation of less than 0.5 in population samples. One-way ANOVA was used to find

statistically significant differences among probes (p-values corrected with Benjamini-Hochberg false discovery method set at $p < 0.05$). All DC subsets were arranged by a hierarchical clustering algorithm using normalized intensity values and based on 2-fold change or greater of all genes ($n=8601$). Heat maps for the differential expressions of core DCs relative to macrophages (two-fold) were generated and analyzed (Figure 6C). For selected DC genes of interest, heat maps were generated (Figure 6D) of normalized intensity values.

Flow cytometry and gating

Cells were stained on ice in PBS with 2.0% (vol/vol) FCS. LSR II (Becton Dickinson) was used for multiparametric flow cytometry of stained cell suspensions, followed by analysis with FlowJo software (TreeStar).

Antibodies, live/dead dye, CFSE, FITC painting and staining reagents

The following reagents were from BD Biosciences, eBioscience or Biolegend: anti-Langerin (eBioL31), anti-CD11c (N418), anti-CD4 (RM4-5), anti-CD8 α (53-6.7), anti-CD11b (M1/70), anti-CD103 (2E7), anti-Armenian Hamster IgG Isotype Control (eBio299Arm), anti-rat IgG2a Isotype Control (eBR2a), anti-CD3 (500A2), anti-CD45 (30-F11), anti-CD205 (NLDC-145), anti-EPCAM (G8.8), anti-CD24 (M1/69), anti-F4/80 (BM8), anti-CD115 (AFS98), anti-PDCA1 (ebio927), anti-Ly6c (HK1.4), anti-B220 (RA3-6B2), anti-I-A/I-E (M5/114.15.2), anti-CD3 (17A2), anti-CD19 (eBio1D3), anti-NK1.1 (PK136). AQUA (L34957) was from Invitrogen. Cytofix/cytoperm kit was from BD Biosciences. CFSE was from Sigma. Anti-CD205 (NLDC-145) was produced in the Steinman lab and conjugated to Alexafluor 488 or 647. Other reagents included PBS and FBS (Gibco-BRL), ACK lysing buffer (BioSource). Staining with anti-Langerin and anti-CD205 was performed with cell surface and intracellular label as described (Cheong *et al.*, 2007). For intracellular blocking 2% rat serum was diluted into perm/wash buffer. All extracellular staining was performed in ice cold PBS with 2% FCS. FITC painting was performed on the flank with 1:1 1% FITC in acetone:Dibutyl phthalate (.5% FITC final) for 16–30 hours prior to harvest.

OVA presentation—Endotoxin free ($< .001\text{EU}/\mu\text{g}$) OVA was purchased from Hyglos. For all groups, equal total numbers of DC subsets and CFSE labeled T cells were cultured at a 1:10 ratio with increasing concentrations of soluble OVA protein.

MLR—Allo-MLR was performed as previously described (Anandasabapathy *et al.*, 2011) from FACS sorted LN resident and migDC subsets isolated from the skin draining LN.

Supplementary Material

Refer to Web version on PubMed Central for supplementary material.

Acknowledgments

We are deeply grateful to Ralph M. Steinman for his mentorship, support, and wisdom. We are grateful to Tibor Keler and Celldex therapeutics for use of recombinant Flt3L, Andrew Sikora, and Paola Longhi for critical reading of the manuscript, Jim Krueger for mentorship, Judy Adams for assistance with figure graphics, and Klara Velinzon for assistance with flow sorting. N.A. was supported in part by grant UL1TR000043/ KL2TR000151 from the

National Center for Research Resources and the National Center for Advancing Translational Sciences (NCATS), National Institutes of Health, the Dermatology Foundation, the Klarman Family Foundation and supported by NIH grants AI40045, 81677, and 13013 (to R.M.S) and NIAMS AR063461-01A1 (to N.A.). C.C. is supported by the grant from the Canadian Institutes of Health Research (CIHR) and Chercheur-Boursier Junior of Fonds de recherche du Québec-Santé (FRSQ). S.T. is supported by NIAMS 5T32AR007098-39. We thank the Harvard Neurobiology Department and the Neurobiology Imaging Facility for consultation and instrument availability that supported this work. This facility is supported in part by the Neural Imaging Center as part of an NINDS P30 Core Center grant #NS072030.

Abbreviations

DC	dendritic cells
migDC	migratory dendritic cells
LN	lymph node
Flt3L	Fms-like tyrosine kinase 3-ligand
PDC	plasmacytoid DC
cDC	classical DC
PCA	principal component analysis

REFERENCES

- Anandasabapathy N, Victora GD, Meredith M, Feder R, Dong B, Kluger C, et al. Flt3L controls the development of radiosensitive dendritic cells in the meninges and choroid plexus of the steady-state mouse brain. *J Exp Med*. 2011; 208:1695–1705. [PubMed: 21788405]
- Bar-On L, Birnberg T, Lewis KL, Edelson BT, Bruder D, Hildner K, et al. CX3CR1+ CD8alpha+ dendritic cells are a steady-state population related to plasmacytoid dendritic cells. *Proc Natl Acad Sci U S A*. 2010; 107:14745–14750. [PubMed: 20679228]
- Bedoui S, Whitney PG, Waithman J, Eidsmo L, Wakim L, Caminschi I, et al. Crosspresentation of viral and self antigens by skin-derived CD103+ dendritic cells. *Nat Immunol*. 2009; 10:488–495. [PubMed: 19349986]
- Bozzacco L, Trumpfheller C, Huang Y, Longhi MP, Shimeliovich I, Schauer JD, et al. HIV gag protein is efficiently cross-presented when targeted with an antibody towards the DEC-205 receptor in Flt3 ligand-mobilized murine DC. *Eur J Immunol*. 2010; 40:36–46. [PubMed: 19830741]
- Cheong C, Idoyaga J, Do Y, Pack M, Park SH, Lee H, et al. Production of monoclonal antibodies that recognize the extracellular domain of mouse Langerin/CD207. *J Immunol Methods*. 2007; 324:48–62. [PubMed: 17553520]
- Cheong C, Matos I, Choi JH, Dandamudi DB, Shrestha E, Longhi MP, et al. Microbial stimulation fully differentiates monocytes to DC-SIGN/CD209(+) dendritic cells for immune T cell areas. *Cell*. 2010; 143:416–429. [PubMed: 21029863]
- Choi JH, Cheong C, Dandamudi DB, Park CG, Rodriguez A, Mehandru S, et al. Flt3 signaling-dependent dendritic cells protect against atherosclerosis. *Immunity*. 2011; 35:819–831. [PubMed: 22078798]
- Clark RA. Skin-resident T cells: the ups and downs of on site immunity. *J Invest Dermatol*. 2010; 130:362–370. [PubMed: 19675575]
- Esche C, Subbotin VM, Hunter O, Peron JM, Maliszewski C, Lotze MT, et al. Differential regulation of epidermal and dermal dendritic cells by IL-12 and Flt3 ligand. *J Invest Dermatol*. 1999; 113:1028–1032. [PubMed: 10594747]
- Flacher V, Tripp CH, Haid B, Kissenpfennig A, Malissen B, Stoitzner P, et al. Skin langerin+ dendritic cells transport intradermally injected anti-DEC-205 antibodies but are not essential for subsequent cytotoxic CD8+ T cell responses. *J Immunol*. 2012; 188:2146–2155. [PubMed: 22291181]

- Forster R, Schubel A, Breitfeld D, Kremmer E, Renner-Muller I, Wolf E, et al. CCR7 coordinates the primary immune response by establishing functional microenvironments in secondary lymphoid organs. *Cell*. 1999; 99:23–33. [PubMed: 10520991]
- Ginhoux F, Liu K, Helft J, Bogunovic M, Greter M, Hashimoto D, et al. The origin and development of nonlymphoid tissue CD103+ DCs. *J Exp Med*. 2009; 206:3115–3130. [PubMed: 20008528]
- Ginhoux F, Ng LG, Merad M. Understanding the murine cutaneous dendritic cell network to improve intradermal vaccination strategies. *Curr Top Microbiol Immunol*. 2012; 351:1–24. [PubMed: 21058006]
- Haniffa M, Shin A, Bigley V, McGovern N, Teo P, See P, et al. Human tissues contain CD141hi cross-presenting dendritic cells with functional homology to mouse CD103+ nonlymphoid dendritic cells. *Immunity*. 2012; 37:60–73. [PubMed: 22795876]
- Helft J, Ginhoux F, Bogunovic M, Merad M. Origin and functional heterogeneity of non-lymphoid tissue dendritic cells in mice. *Immunol Rev*. 2010; 234:55–75. [PubMed: 20193012]
- Helft J, Manicassamy B, Guernonprez P, Hashimoto D, Silvén A, Agudo J, et al. Crosspresenting CD103+ dendritic cells are protected from influenza virus infection. *J Clin Invest*. 2012; 122:4037–4047. [PubMed: 23041628]
- Henri S, Poulin LF, Tamoutounour S, Ardouin L, Guillems M, de Bovis B, et al. CD207+ CD103+ dermal dendritic cells cross-present keratinocyte-derived antigens irrespective of the presence of Langerhans cells. *J Exp Med*. 2010; 207:189–206. [PubMed: 20038600]
- Igyarto BZ, Haley K, Ortner D, Bobr A, Gerami-Nejad M, Edelson BT, et al. Skinresident murine dendritic cell subsets promote distinct and opposing antigen-specific T helper cell responses. *Immunity*. 2011; 35:260–272. [PubMed: 21782478]
- Jung S, Aliberti J, Graemmel P, Sunshine MJ, Kreutzberg GW, Sher A, et al. Analysis of fractalkine receptor CX(3)CR1 function by targeted deletion and green fluorescent protein reporter gene insertion. *Mol Cell Biol*. 2000; 20:4106–4114. [PubMed: 10805752]
- Kase K, Hua J, Yokoi H, Ikeda K, Nagaoka I. Inhibitory action of roxithromycin on histamine release and prostaglandin D2 production from beta-defensin 2-stimulated mast cells. *Int J Mol Med*. 2009; 23:337–340. [PubMed: 19212651]
- Kenney RT, Frech SA, Muenz LR, Villar CP, Glenn GM. Dose sparing with intradermal injection of influenza vaccine. *N Engl J Med*. 2004; 351:2295–2301. [PubMed: 15525714]
- Kissenpfennig A, Henri S, Dubois B, Laplace-Builhe C, Perrin P, Romani N, et al. Dynamics and function of Langerhans cells in vivo: dermal dendritic cells colonize lymph node areas distinct from slower migrating Langerhans cells. *Immunity*. 2005; 22:643–654. [PubMed: 15894281]
- Liu K, Vitorica GD, Schwickert TA, Guernonprez P, Meredith MM, Yao K, et al. In vivo analysis of dendritic cell development and homeostasis. *Science*. 2009; 324:392–397. [PubMed: 19286519]
- Liu L, Zhong Q, Tian T, Dubin K, Athale SK, Kupper TS. Epidermal injury and infection during poxvirus immunization is crucial for the generation of highly protective T cell-mediated immunity. *Nat Med*. 2010; 16:224–227. [PubMed: 20081864]
- Manfra DJ, Chen SC, Jensen KK, Fine JS, Wiekowski MT, Lira SA. Conditional expression of murine Flt3 ligand leads to expansion of multiple dendritic cell subsets in peripheral blood and tissues of transgenic mice. *J Immunol*. 2003; 170:2843–2852. [PubMed: 12626534]
- Martin-Fontecha A, Baumjohann D, Guarda G, Reboldi A, Hons M, Lanzavecchia A, et al. CD40L+ CD4+ memory T cells migrate in a CD62P-dependent fashion into reactive lymph nodes and license dendritic cells for T cell priming. *J Exp Med*. 2008; 205:2561–2574. [PubMed: 18838544]
- Martin-Fontecha A, Sebastiani S, Hopken UE, Uguccioni M, Lipp M, Lanzavecchia A, et al. Regulation of dendritic cell migration to the draining lymph node: impact on T lymphocyte traffic and priming. *J Exp Med*. 2003; 198:615–621. [PubMed: 12925677]
- Merad M, Sathe P, Helft J, Miller J, Mortha A. The dendritic cell lineage: ontogeny and function of dendritic cells and their subsets in the steady state and the inflamed setting. *Annu Rev Immunol*. 2013; 31:563–604. [PubMed: 23516985]
- Meredith MM, Liu K, Darrasse-Jeze G, Kamphorst AO, Schreiber HA, Guernonprez P, et al. Expression of the zinc finger transcription factor zDC (Zbtb46, Btbd4) defines the classical dendritic cell lineage. *J Exp Med*. 2012a; 209:1153–1165. [PubMed: 22615130]

- Meredith MM, Liu K, Kamphorst AO, Idoyaga J, Yamane A, Guermonprez P, et al. Zinc finger transcription factor zDC is a negative regulator required to prevent activation of classical dendritic cells in the steady state. *J Exp Med*. 2012b; 209:1583–1593. [PubMed: 22851594]
- Miller JC, Brown BD, Shay T, Gautier EL, Jojic V, Cohain A, et al. Deciphering the transcriptional network of the dendritic cell lineage. *Nat Immunol*. 2012; 13:888–899. [PubMed: 22797772]
- Naik SH, Proietto AI, Wilson NS, Dakic A, Schnorrer P, Fuchsberger M, et al. Cutting edge: generation of splenic CD8⁺ and CD8⁻ dendritic cell equivalents in Fms-like tyrosine kinase 3 ligand bone marrow cultures. *J Immunol*. 2005; 174:6592–6597. [PubMed: 15905497]
- Poulin LF, Salio M, Griessinger E, Anjos-Afonso F, Craciun L, Chen JL, et al. Characterization of human DNGR-1⁺ BDCA3⁺ leukocytes as putative equivalents of mouse CD8 α ⁺ dendritic cells. *J Exp Med*. 2010; 207:1261–1271. [PubMed: 20479117]
- Satpathy AT, Kc W, Albring JC, Edelson BT, Kretzer NM, Bhattacharya D, et al. Zbtb46 expression distinguishes classical dendritic cells and their committed progenitors from other immune lineages. *J Exp Med*. 2012; 209:1135–1152. [PubMed: 22615127]
- Schon MP, Schon M. TLR7 and TLR8 as targets in cancer therapy. *Oncogene*. 2008; 27:190–199. [PubMed: 18176600]
- Seillet C, Jackson JT, Markey KA, Brady HJ, Hill GR, Macdonald KP, et al. CD8 α ⁺ DCs can be induced in the absence of transcription factors Id2, Nfil3, and Batf3. *Blood*. 2013; 121:1574–1583. [PubMed: 23297132]
- Seneschal J, Jiang X, Kupper TS. Langerin⁺ Dermal DC, but not Langerhans Cells, are Required for Effective CD8 Mediated Immune Responses after Skin Scarification with Vaccinia Virus (VACV). *J Invest Dermatol*. 2013
- Shortman K, Heath WR. The CD8⁺ dendritic cell subset. *Immunol Rev*. 2010; 234:18–31. [PubMed: 20193009]
- Steinman RM, Kaplan G, Witmer MD, Cohn ZA. Identification of a novel cell type in peripheral lymphoid organs of mice. Purification of spleen dendritic cells, new surface markers, and maintenance in vitro. *J Exp Med*. 1979; 149:1–16. [PubMed: 762493]
- Teunissen MB, Haniffa M, Collin MP. Insight into the immunobiology of human skin and functional specialization of skin dendritic cell subsets to innovate intradermal vaccination design. *Curr Top Microbiol Immunol*. 2012; 351:25–76. [PubMed: 21833835]
- Yamazaki S, Dudziak D, Heidkamp GF, Fiorese C, Bonito AJ, Inaba K, et al. CD8⁺ CD205⁺ splenic dendritic cells are specialized to induce Foxp3⁺ regulatory T cells. *J Immunol*. 2008; 181:6923–6933. [PubMed: 18981112]

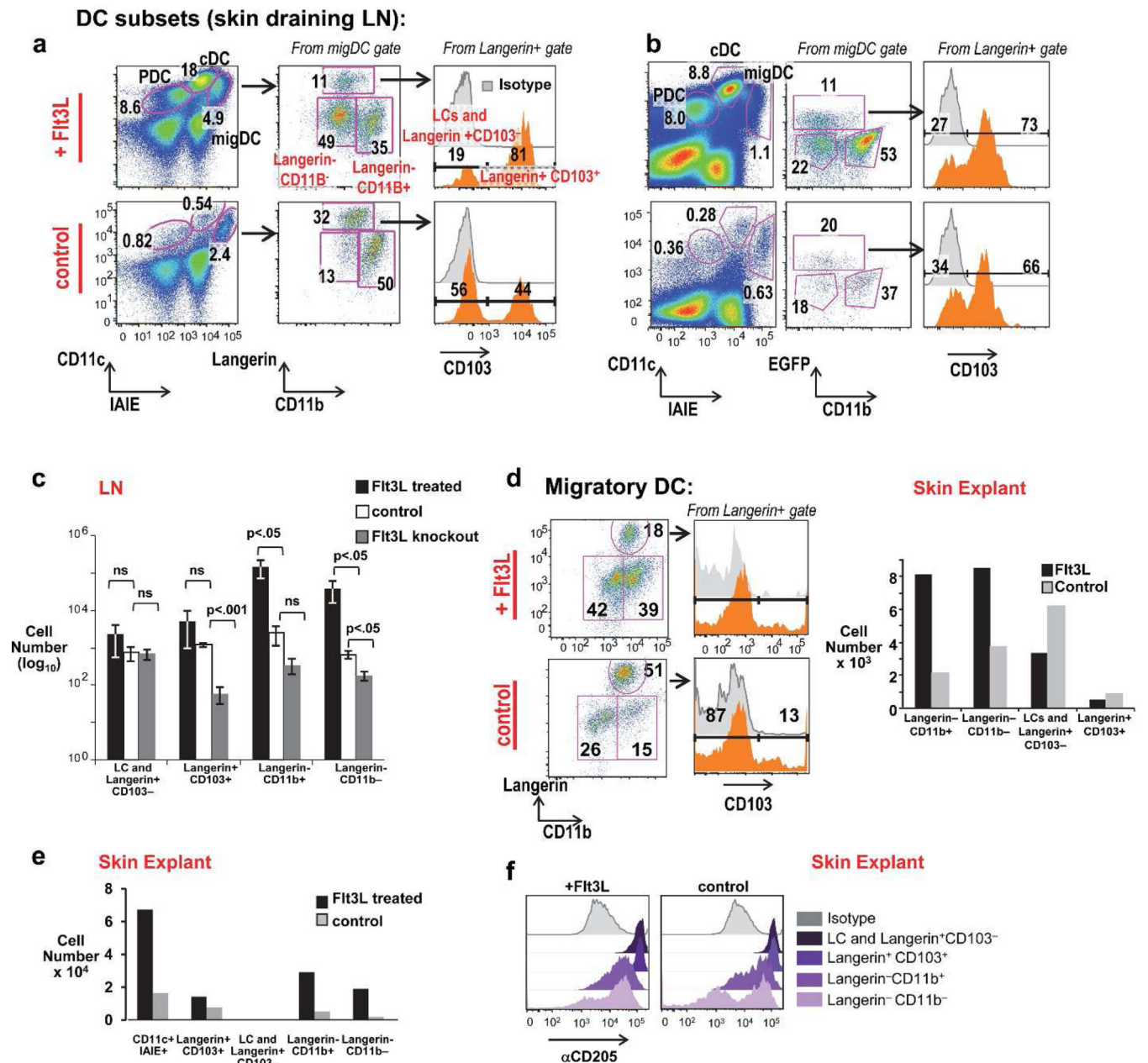


Figure 1. Flt3L dependence of migratory DC subsets, including Langerin-CD11b- DC

A) Schema of LN DC from Flt3L-tumor treated vs. C57Bl/6 (B6) control mice at day 13. PDC (plasmacytoid DC), cDC (classical LN resident DC), migDC (migratory DC) are labeled. (B) LN DC subsets Flt3L-treated (upper) vs. untreated Langerin-GFP mice. (C) Quantitation of migratory DC from Flt3L-treated, control, Flt3L^{-/-} mice (quantitated per skin draining LN; error bars show mean \pm SD of 3 individual mice per group, analyzed by an unpaired t-test). (D) Flt3L-induced expansion of skin resident DC subsets from "crawl-out" skin explants of doxycycline-inducible Flt3L mice given 8 days of doxycycline in their drinking water (top) vs. untreated controls (bottom) (one representative experiment of two). (E) Quantitation of DC isolated from skin explants "crawlouts" of Flt3L-treated vs. control Langerin GFP reporter mice (pooled from the ears of 3 mice per experiment, one representative experiment of three). (F) α CD205+ staining of skin DC subsets from explant cultures of doxycycline treated (Flt3L+) vs. untreated (control) mice (pooled from n=2 mice per condition).

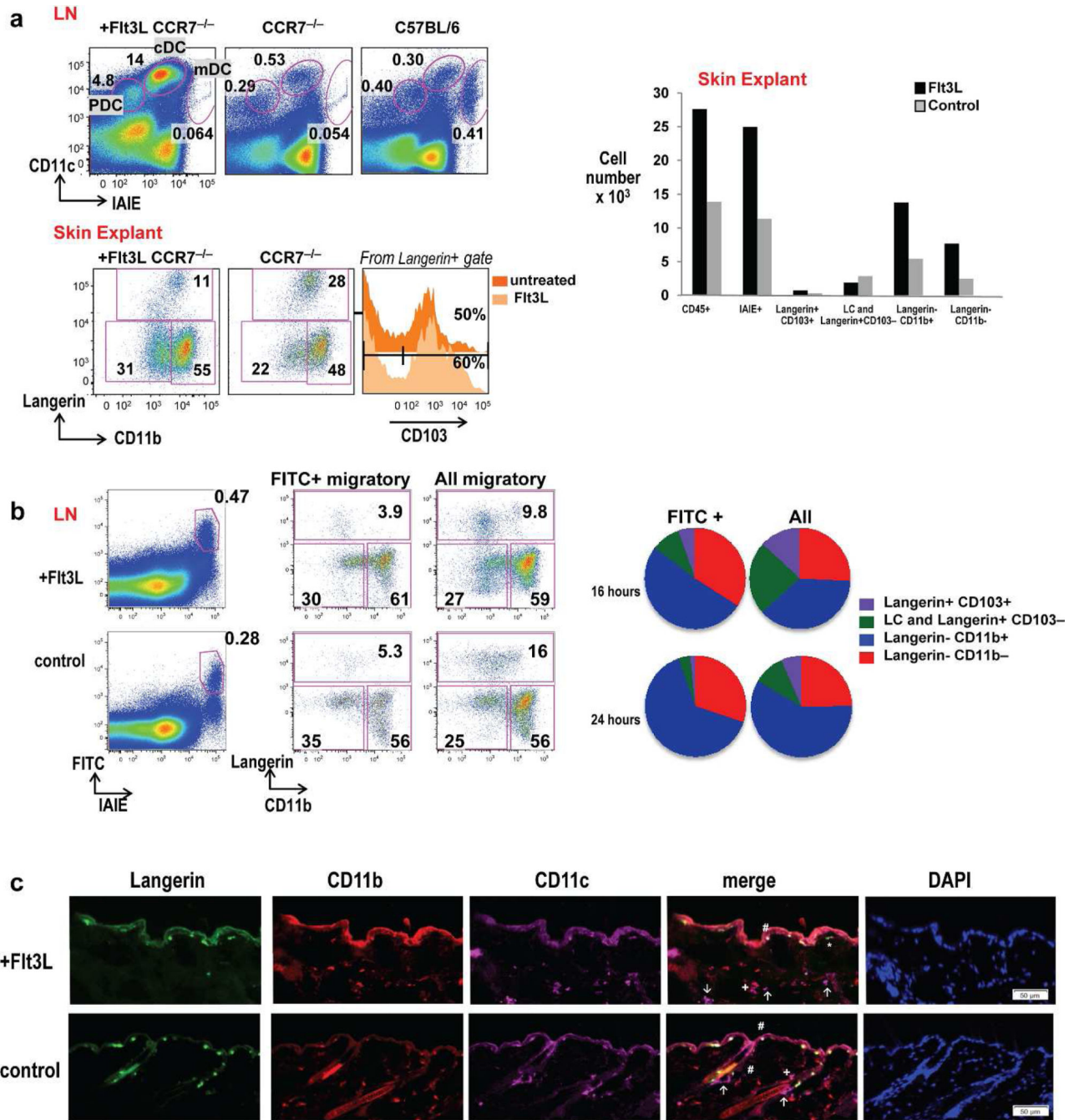


Figure 2. CD11b⁻ DC are skin-resident and migrate to the skin draining LN

(A) Upper: Representative skin draining LN DC gating from CCR7^{-/-} mice treated with Flt3L (left), CCR7^{-/-} untreated controls (middle), and B6 controls (right). Lower: CCR7^{-/-} skin resident DC subsets from “crawl-out” explants (Flt3L treated vs. untreated controls). One of three representative experiments are shown. (B) FITC painting assay with gating on FITC⁺ migratory DC vs. total migratory DC in Flt3L treated (upper) and control mice (lower). CD11b⁻ migDC (red) directly capture FITC in the skin and traffic to the skin draining LN at 16 hour and 24 hours in C57BL6/WT mice (n=3 mice per time point). (C) Immunofluorescence of flank sections of Flt3L-treated (upper) and control (lower) mice co-stained with langerin (green), CD11b (red) and CD11c (magenta) and counterstained with DAPI to visualize cell nuclei. Positions of Langerhans cells (LC:

langerin+, CD11b+, CD11c+, #). Dermal DC (CD11c+) were further distinguished as langerin-CD11b- (\uparrow), langerin-CD11b+ (+) and langerin+CD11b- (*) were marked in the merged images. Scale bar =50 μ m for all images.

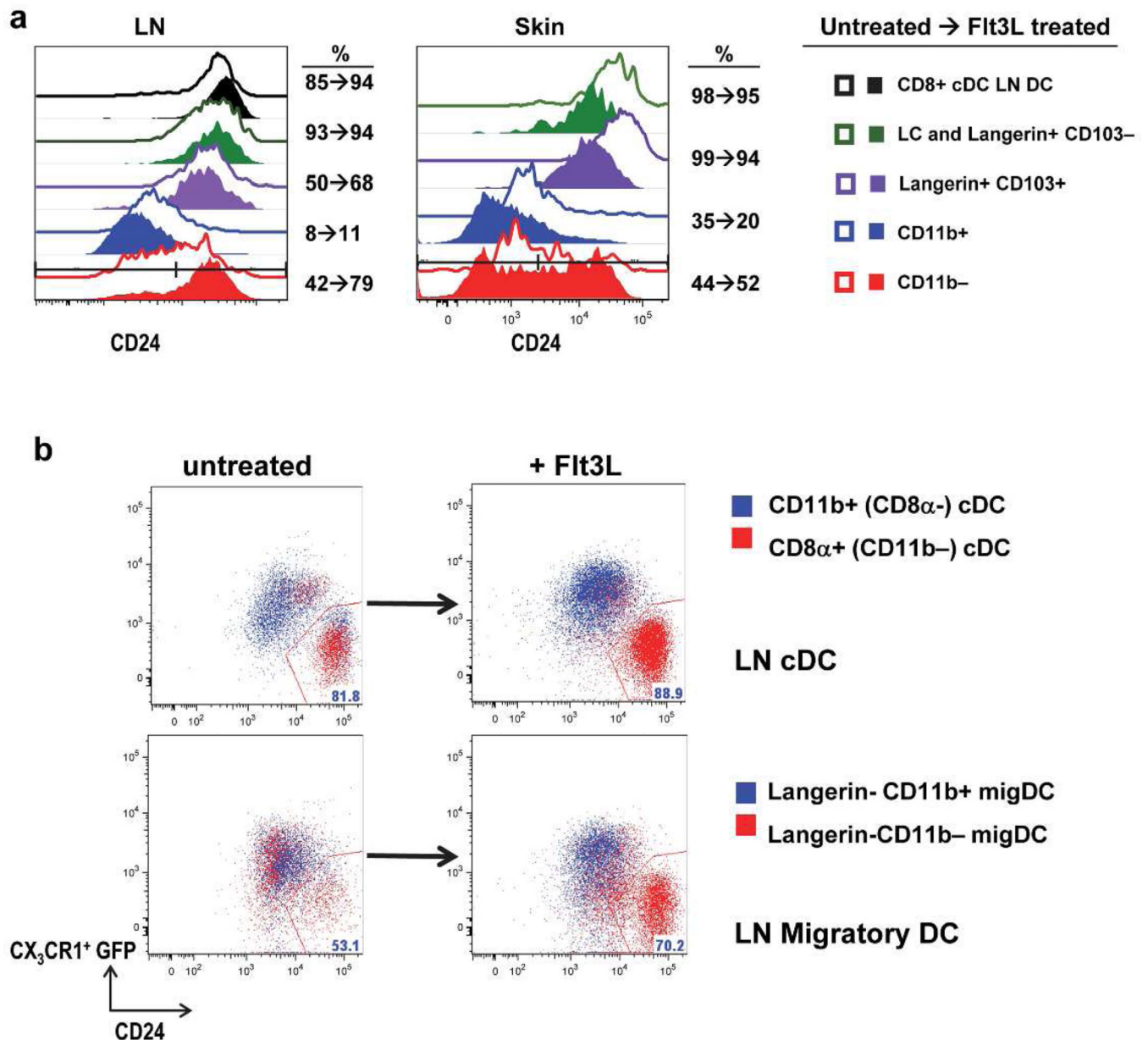


Figure 3. Flt3L responsive CD11b- migDC include CD24^{high} CX₃CR1^{low} subsets

(A) In skin and skin draining LN a subset of CD11b- migDC are CD24⁺ and expand with Flt3L. Gated pre (open) and post (closed) Flt3L in LN and skin explant (lower) as compared to classical CD8α⁺ + DC and other migDC (n=3 mice per group, one representative experiment of three). (B) Lower: Flt3L expanded CD24⁺ cells are CX₃CR1^{low} within the CD11b- migDC subset (red) as compared to migratory CD11b⁺ cells (blue). Upper: Comparison of LN resident CD11b⁺ CD8α⁻ cDC (blue) and CD8α⁺ + cDC which are CD24⁺ CX₃CR1^{low} (red) (n=2 Flt3L-treated or control CX₃CR1 mice per group, one representative experiment of two).

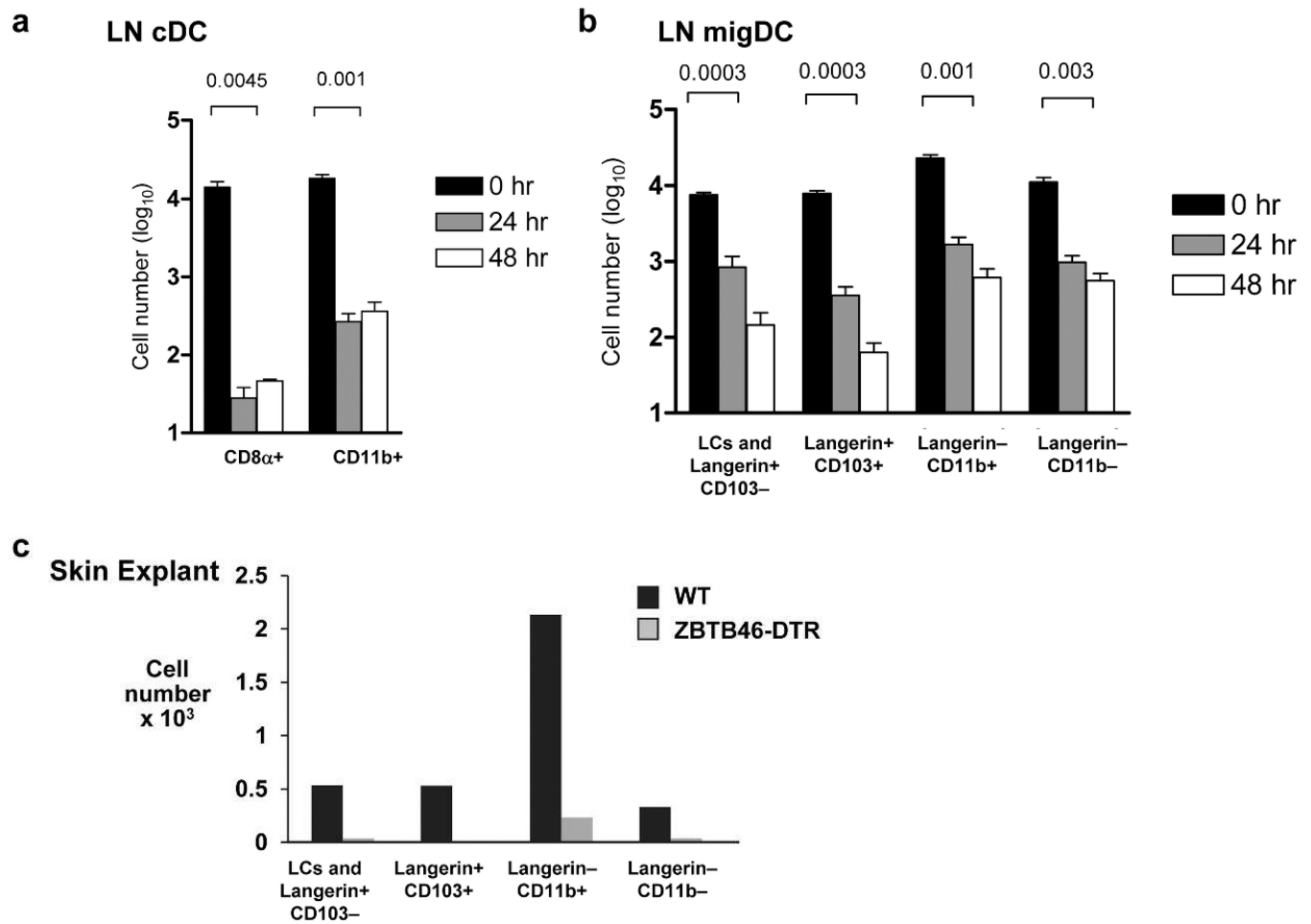


Figure 4. CD11b⁻ migDC are Zbtb46 dependent

(A) LN classical vs. total migratory DC and (B) migratory DC subset counts from skin draining LNs after single dose DT vs. PBS administration 24 or 48 hours prior to harvest (n=3 mice per time point, one representative experiment of three). (C) Skin explants pooled from three Zbtb46DTR vs. C57BL/6 controls 24 hours after DT treatment (n=3 mice pooled per group, one representative experiment of two).

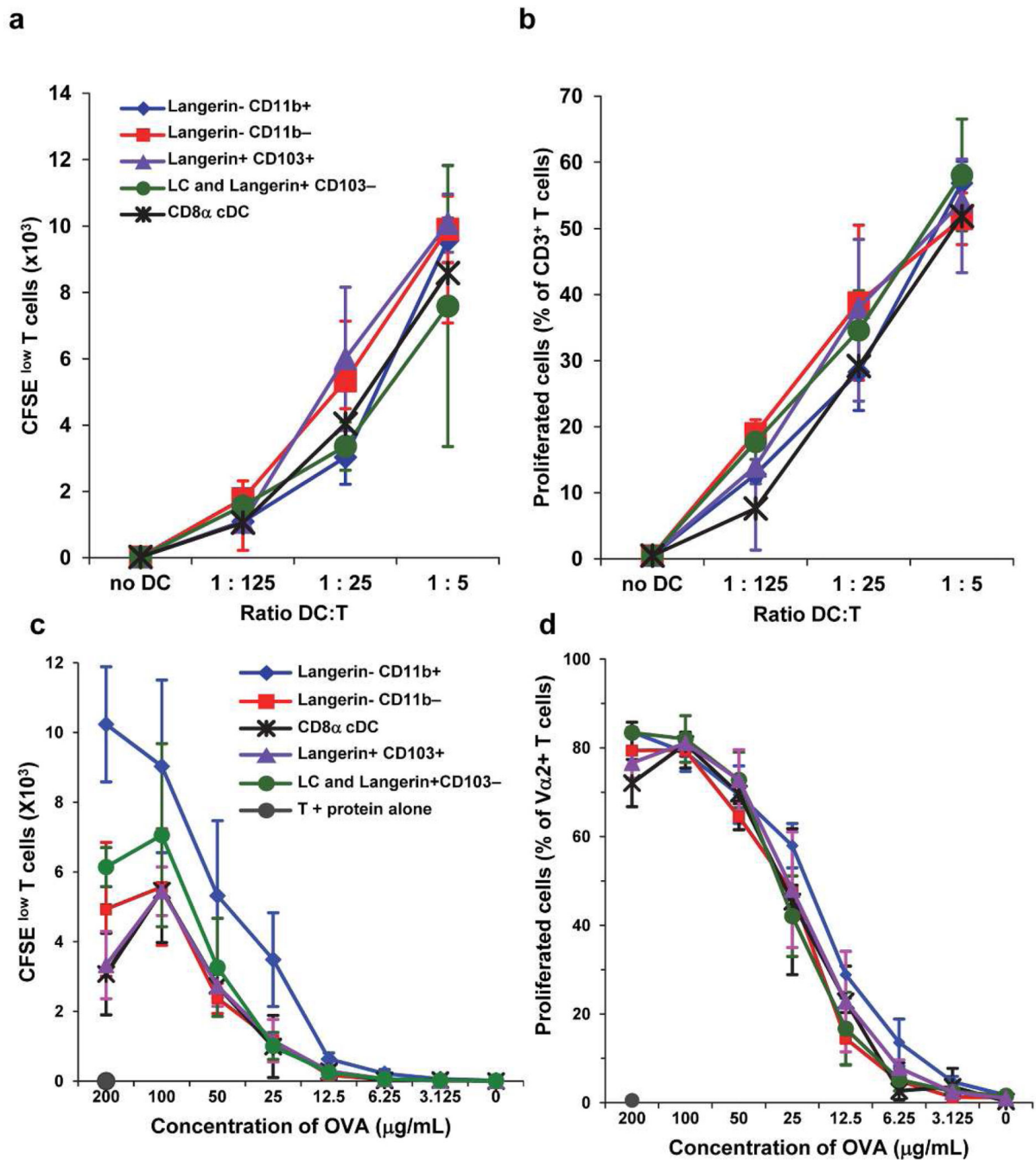
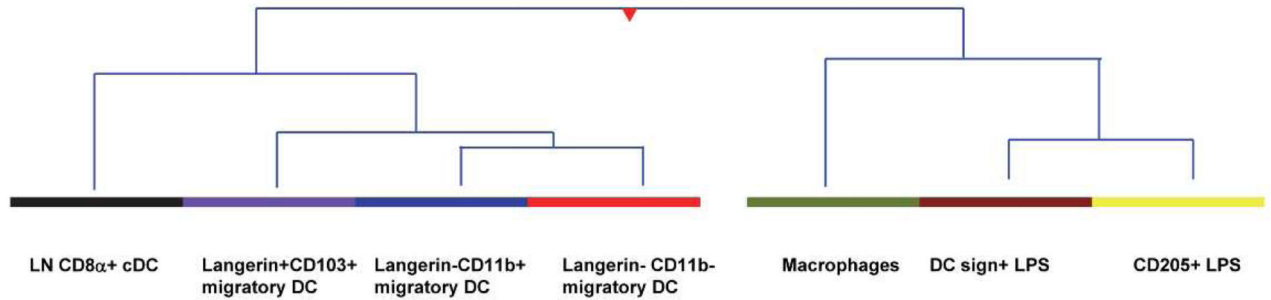
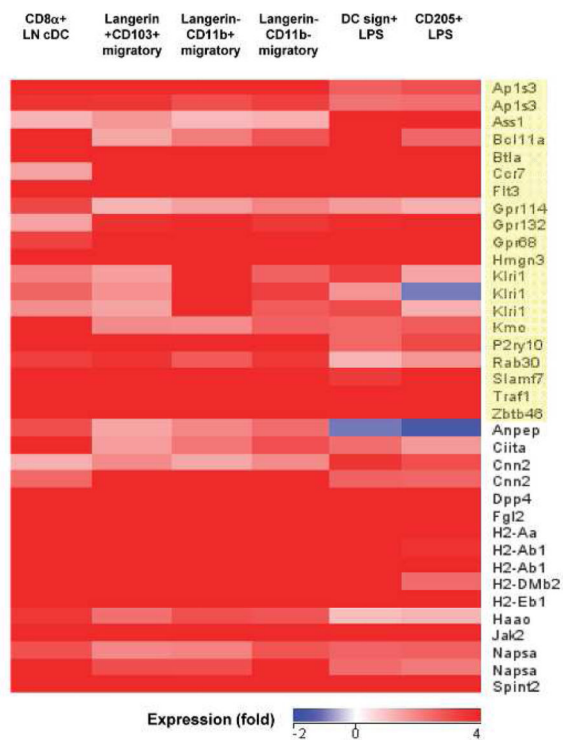
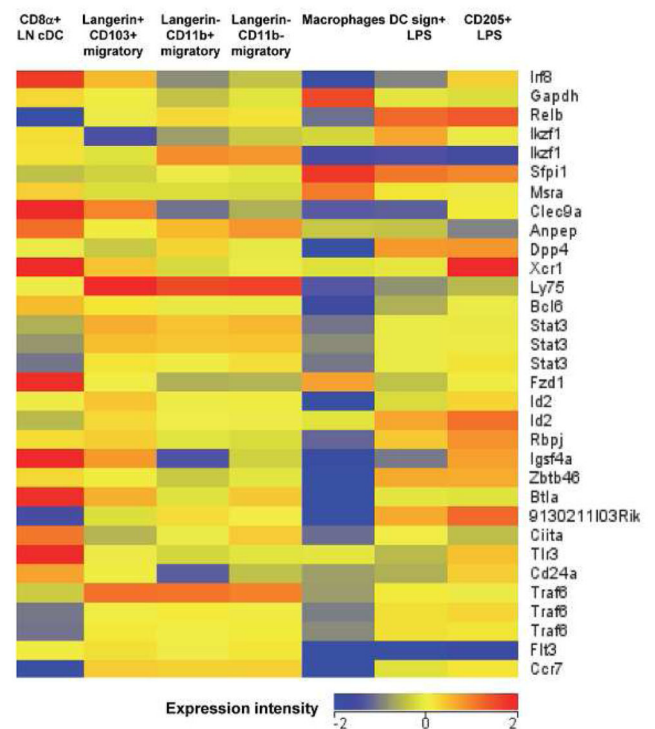


Figure 5. CD11b- migDC present antigen

CD11b- migDC present antigen CD11b- migDC present allo-antigens in the mixed leukocyte reaction (A-B) and present OVA protein (C-D) to CD8+ V α 2 OT-1 T cells with equal efficiency to other DC subsets *ex vivo*. One of two duplicate experiments are shown with triplicate wells per sample.

a Hierarchy cluster**b****c****Figure 6. Langerin- CD11b- DC relate closely to classical DC**

(A) Hierarchical clustering of subsets based on 2 fold change or greater of all genes (n=8601) (B) Heat map comparison of DC signature gene expression across DC groups as compared to macrophages (yellow indicates the core DC signature). (C) Heat map comparison of normalized intensity values from selected DC genes across all subsets.